Syntheses, Structures, and Molecular Orbital Analysis of Hydridotris(pyrazolyl)borate (Tp) Molybdenum Carbonyls: Paramagnetic $TpMo(CO)_3$ and Triply Bonded $Tp_2Mo_2(CO)_4$ (Mo≡Mo)[1]

M. David Curtis,* Kom-Bei Shiu, W. M. Butler, and John C. Huffman[†]

Contribution from the Department of Chemistry, The University of Michigan, Ann Arbor, Michigan 48109, and the Indiana University Molecular Structure Center, Bloomington, Indiana 47405. *Received February 26, 1985*

Abstract: Tris(pyrazolyl)borate ion, $HB(C_3N_2H_3)_3^-$ (Tp), reacts with $Mo(CO)_6$ to give the anion, $TpMo(CO)_3^-$, which in turn is easily oxidized to the paramagnetic radical, $TpMo(CO)_3$ (**1**), by a variety of mild oxidizing agents, e.g., Cp_2Fe^+. EHMO and ^1H NMR studies of **1** show the odd electron occupies a doubly degenerate oribtal and that the odd electron is delocalized onto the pyrazolyl rings of the Tp ligand by π-bonding. The bonding of Tp and Cp ligands is compared in light of the EHMO results. Decarbonylation of **1** gives the triply bonded complex, $Tp_2Mo_2(CO)_4$ (Mo≡Mo) (**2**). Compound **2** is largely unreactive toward nucleophiles, and the Mo≡Mo triple bond is cleaved in reaction with Br_2, S_8, etc. Several attempts to prepare mixed ligand dimers of the type $TpCpMo_2(CO)_n$ are described. Compound **1** crystallizes in the trigonal system: space group $P\bar{3}$, $Z = 2$, $a = b = 11.359$ (4) Å, $c = 8.161$ (2) Å, $V = 911.9$ (3) Å^3. The refinement converged with R_1, $R_2 = 0.0383$, 0.0435 based on 440 reflections with $I > 2.33\sigma(I)$. The molecule has strict C_3 symmetry with Mo–N = 2.207 (7) Å, Mo–C = 2.013 (11) Å, C–O = 1.126 (11) Å, C–Mo–N = 94.8 (3)°, C–Mo–C = 87.8 (4)°, and N–Mo–N = 82.5 (3)°. The structure of **2** was determined on a solvate, **2**·$CHCl_3$, which crystallized in the orthorhombic system, space group *Pbca*, $Z = 8$, a, b, c = 12.995 (2), 16.974 (4), 29.396 (6) Å, $V = 6485$ (2) Å^3. The refinement, based on 2957 reflections with $I > 3\sigma(I)$, converged with R_1, $R_2 = 0.055$, 0.063. The molecule has approximate C_2 symmetry. The N-donor atoms are in two general locations, one trans to the Mo≡Mo bond (Mo–N = 2.21 [1] Å) and one cis to the Mo≡Mo bond and trans to the carbonyls (Mo–N = 2.23 [1] Å). The carbonyls are also divided into two sets, one semibridging (Mo–C = 1.93 [1] Å, Mo–Mo–C = 70.5 [1.5]°) and one terminal (Mo–C = 1.96 [1] Å, Mo–Mo–C = 83.4 [4]°). The Mo≡Mo bond length is 2.507 (1) Å.

The Mo≡Mo triple bond in $Cp_2Mo_2(CO)_4$ displays a rich chemistry toward both nucleophilic and electrophilic reagents.[2] The objective of our research in this area is the systematic development of the reactivity of metal–metal triple bonds with the ultimate goal of developing reactivity rules so that metal–metal bonds might be regarded as "inorganic functional groups" for the elaboration of more complex structures.

A comparison of the chemistry of $Cp_2Mo_2(CO)_4$ and $Cp^*_2Mo_2(CO)_4$ ($Cp = \eta^5$-C_5H_5, $Cp^* = \eta^5$-C_5Me_5) shows both similarities and dissimilarities.[2,3] Likewise, the compounds, Mo_2X_6 (X = RO, R_2N), have a diverse and interesting chemistry which, while showing parallels with that of $Cp_2Mo_2(CO)_4$, is quite different in detail as a result of the different electron configurations.[4] Thus, the formally 12-electron Mo_2X_6 species are stabilized by π-donor ligands (e.g., OR, NR_2) whereas the 18-electron $Cp_2Mo_2(CO)_4$ is stabilized by π-acid CO ligands. The former may add nucleophiles without a concomitant reduction in metal–metal bond order, but a reduction in bond order from 3 to 2 or 1 accompanies the addition of donors to the latter.[2]

If reactivity patterns *specific* to a particular metal–metal multiple bond with a given electron configuration are to be derived, then the reactivity of such a bond with various supporting ligands must also be investigated in order to separate, *if possible*, steric and electronic effects of the ligands from the reactivity inherent in the metal–metal unsaturation. For this reason, we undertook the synthesis of $Tp_2Mo_2(CO)_4$(Mo≡Mo) (Tp = hydridotris(pyrazolyl)borate, $HB(C_3H_3N_2)_3^-$). The steric bulk of the Tp ligand resembles that of the Cp* ligand, but it was anticipated that the electronic properties of Tp would be quite unlike those of Cp* or Cp. The question was the following: how would these differences be manifested in the reactivity of a Mo≡Mo triple bond?

The different electronic and steric properties of Tp vs. Cp or Cp* are manifested in several ways. First, there is a paucity of seven-coordinate complexes of the type $TpMoL_4$, whereas the 4-legged piano stool geometry is ubiquitous in $CpMoL_4$ complexes. The Tp ligand clearly prefers six-coordination even though the resulting complexes often achieve only a 16-electron count.[5-7] Second, the Cp and Cp* ligands support an extensive array of metal–metal bonded dimers and clusters, but previous to the

[†] Molecular Structure Center.

(1) Metal–Metal Multipl Bonds; Part 17. Part 16: D'Errico, J. J.; Curtis, M. D. *J. Am. Chem. Soc.* **1983**, *105*, 4479.

(2) Reviews: (a) Curtis, M. D.; Messerle, L.; Fotinos, N. A.; Gerlach, R. F. *ACS Symp. Ser.* **1981**, *155*, 221–257. (b) Cotton, F. A.; Walton, R. A. *Multiple Bonds Between Metal Atoms*; Wiley: New York, 1982. Reactions with diazoalkanes: (c) Messerle, L.; Curtis, M. D. *J. Am. Chem. Soc.* **1982**, *104*, 889. (d) D'Errico, J. J.; Messerle, L.; Curtis, M. D. *Inorg. Chem.* **1983**, *22*, 849. (e) Herrmann, W. A. *Adv. Organomet. Chem.* **1982**, *20*, 160–252. Metal cluster formation: (f) Williams, P. D.; Curtis, M. D.; Duffy, D. N.; Butler, W. M. *Organometallics* **1983**, *2*, 165. (g) Green, M.; Porter, S. J.; Stone, F. G. A. *J. Chem. Soc., Dalton Trans.* **1983**, 513. (h) Cotton, F. A.; Schwotzer, W. *Angew. Chem., Int. Ed. Engl.* **1982**, *21*, 629. (i) Brun, P.; Dawkins, G. M.; Green, M.; Miles, A. D.; Orpen, A. G.; Stone, F. G. A. *J. Chem. Soc., Chem. Commun.* **1982**, 926. (j) Bernal, I.; Brunner, H.; Meier, W.; Pfisterer, H.; Wachter, J.; Ziegler, M. L. *Angew. Chem., Int. Ed. Engl.* **1984**, *23*, 438. Reactions with organosulfur compounds: (k) Alper, H.; Einstein, F. W. B.; Petrignani, J.-F.; Willis, A. C. *Organometallics* **1982**, *2*, 1422. (l) Alper, H.; Einstein, F. W. B.; Hartstock, F. W.; Willis, A. C. *J. Am. Chem. Soc.* **1985**, *107*, 173. Reaction with H_2: (m) Alt, H. G.; Mahmoud, K. A.; Rest, A. J. *Angew. Chem., Int. Ed. Engl.* **1983**, *22*, 544. (n) Curtis, M. D.; Fotinos, N. A.; Han, K. R.; Butler, W. M. *J. Am. Chem. Soc.* **1983**, *105*, 2686. Reactions with alkynes: (o) Gerlach, R. F.; Duffy, D. N.; Curtis, M. D. *Organometallics* **1983**, *2*, 1172. Micellaneous: (p) Adams, R. D.; Katehira, D. A.; Yang, L.-W. *Organometallics* **1982**, *1*, 231. (q) Brunner, H.; Hoffmann, B.; Wachter, J. *J. Organomet. Chem.* **1983**, *252*, C35. (r) Scherer, O. J.; Sitzmann, H.; Wolmershäuser, G. *J. Organomet. Chem.* **1984**, *268*, C9.

(3) (a) King, R. B.; Efraty, A. *J. Organomet. Chem.* **1973**, *60*, 125. (b) King, R. B.; Iqbal, M. Z.; King, A. D., Jr. *Ibid.* **1979**, *171*, 53. (c) Huang, J.-S.; Dahl, L. F. *Ibid.* **1983**, *243*, 57. (d) Brunner, H.; Meier, W.; Wachter, J. *Ibid.* **1981**, *210*, C23. (e) Buchner, H.; Wachter, J.; Bernall, I.; Ries, W. H. *Ibid.* **1983**, *244*, 247. (f) King, R. B. *Chem. Rev.* **1976**, *20*, 155.

(4) Reviews: (a) Chisholm, M. H. *Transition Met. Chem.* **1978**, *3*, 321. (b) Chisholm, M. H. *Adv. Chem. Ser.* **1979**, *173*, 396. (c) Chisholm, M. H.; Cotton, F. A. *Acc. Chem. Res.* **1978**, *11*, 356. (d) Chisholm, M. H.; Rothwell, I. P. *Prog. Inorg. Chem.* **1982**, *29*, 1. Representative reactions of M_2X_6: (e) Chisholm, M. H.; Hoffman, D. M.; Huffman, J. C. *Inorg. Chem.* **1984**, *23*, 3683. (f) Chisholm, M. H.; Kirkpatrick, C. C.; Huffman, J. C. *Ibid.* **1981**, *20*, 871. (g) Chisholm, M. H.; Huffman, J. C.; Leonelli, J.; Rothwell, I. P. *J. Am. Chem. Soc.* **1982**, *104*, 7030. (h) Chisholm, M. H.; Folting, K.; Huffman, J. C.; Kirkpatrick, C. C.; Ratermann, A. L. *Ibid.* **1981**, *103*, 1305. (i) Chisholm, M. H.; Huffman, J. C.; Marchant, N. S. *Ibid.* **1983**, *105*, 6162. (j) Chisholm, M. H.; Folting, K.; Hoffman, D. M.; Huffman, J. C. *Ibid.* **1984**, *106*, 6794. (k) Strutz, H.; Schrock, R. R. *Organometallics* **1984**, *3*, 1600. (l) Listemann, M. L.; Schrock, R. R. *Ibid.* **1985**, *4*, 74.

0002-7863/86/1508-3335$01.50/0

present work, only only metal–metal bonded dimer of the type $Tp_2M_2L_n$ was known. This compound, $Tp_2Mo_2(OAc)_2$(Mo^{4+} Mo),[8a] was prepared by a substitution of Tp^- on $Mo_2(OAc)_4$ and only two of the three N donors of the Tp ligand are strongly bonded to Mo—the 3rd is weakly bonded in an axial site. During the course of this work, three related Rh complexes, $[RE(pz)_3]_2Rh_2(\mu\text{-}CO)_3$ (R = Me, E = Ga;[8b] and R = H and pz, E = B[8c]), were reported. These confacial, bioctahedral complexes contain Rh–Rh bonds. Thus, our target molecule, $Tp_2Mo_2(CO)_4$, would also represent an unusual complex in poly(pyrazolyl)borate coordination chemistry.

This paper reports the synthesis of $Tp_2Mo_2(CO)_4$ via a paramagnetic monomer, $TpMo(CO)_3$, the structures and some reactions of these compounds, and an EHMO analysis of the bonding in $TpMo(CO)_3$. Portions of this work were communicated in preliminary form.[9]

Experimental Section

All reactions were carried out under N_2 atmosphere by using Schlenk techniques or in an inert atmosphere box equipped with a recirculation/purification train. Solvents were distilled under N_2 from their respective drying agents: (solvent/drying agent) CH_2Cl_2/P_4O_{10}, CH_3CN/CaH_2, THF and diglyme/K–benzophenone, hexane/CaH_2, $CHCl_3/P_4O_{10}$, and toluene/Na–benzophenone. $[Et_4N][TpMo(CO)_3]$,[5] $CpMo(CO)_3BF_4$,[10] $Cp_2Mo_2(CO)_6$,[11] $Cp_2Mo_2(CO)_4$,[11] and Cp_2FePF_6[12] were prepared by published procedures. Elemental analyses were performed by Galbraith Laboratories, Inc. or by Schwartzkopf Microanalytical Laboratories. ^1H and ^{13}C NMR spectra were recorded on a Bruker WM-360 spectrometer. IR spectra were obtained on a Perkin-Elmer Model 1330 instrument calibrated with polystyrene film. The B–H stretch was observed near 2500 cm^{-1}, and the bands associated with the Tp ligand were essentially as observed previously[6] for all compounds reported here. The mass spectrum of $[TpMo(CO)_2]_2S$ was obtained on a Finnegan 4021 quadrupole spectrometer by using chemical ionization (CH_4^+).

$TpMo(CO)_3$ (1). $[Et_4N][TpMo(CO)_3]$ (7.63 g, 14.6 mmol) was added portionwise to a solution of Cp_2FePF_6 (4.83 g, 14.6 mmol) in 100 mL of THF with efficient stirring. After 10 min, the solution was filtered to remove the precipitated Et_4NPF_6, and the solvent was removed from the filtrate under vacuum. The residue was dissolved in 50 mL of CH_2Cl_2, the solution was filtered, and 50 mL of toluene was added to the filtrate. The CH_2Cl_2 was removed slowly under vacuum to give a red-brown solid which was washed with 10 mL of hexane and dried under vacuum. Yield: 4.62 g (80%); mp 189° dec; IR (CH_2Cl_2) 2010 (s), 1885 (br s) cm^{-1}; ^1H NMR (C_6D_6) 3.04, −8.62, −18.94 ppm; ^1H NMR (acetone-d_6) 3.52, −7.69, −17.11 ppm; ^1H NMR ($CDCl_3$) δ 3.08, −8.45, −18.72 ppm. Anal. Calcd for $C_{12}H_{10}BMoN_6O_3$: C, 36.67; H, 2.56. Found: C, 33.81, 33.70; H, 3.83, 3.57. The compound is extremely air sensitive and darkens in air within seconds. The air sensitivity is probably the reason for the low percent C observed in the elemental analysis of **1**. In fact, the analysis obtained (see above) fits closely for $TpMo(CO)_3 \cdot O_2$ (calcd C, 33.91; H, 2.37).

Reaction of $[Et_4N][TpMo(CO)_3]$ and $[CpMo(CO)_3]BF_4$. A solution of $[CpMo(CO)_3]BF_4$ (0.30 g, 0.90 mmol) in 20 mL of CH_2Cl_2 was added dropwise to 0.46 g (0.88 mmol) of $[Et_4N][TpMo(CO)_3]$ dissolved in 50 mL of CH_2Cl_2. After a few min, the IR spectrum of the mixture showed new bands at 2020 (s), 1965 (s), and 1915 (s) cm^{-1}. The solution was concentrated and filtered, and the filtrate was allowed to evaporate slowly in the inert atmosphere box. Some purple crystals formed which were shown to be $Cp_2Mo_2(CO)_6$ by their IR and unit cell parameters.[13] The remaining solvent was then removed under vacuum, and the residue was taken up in $CDCl_3$. The ^1H NMR spectrum showed the presence of $TpMo(CO)_3$ (**1**) and $Cp_2Mo_2(CO)_6$.

$Tp_2Mo_2(CO)_4$ (2). A solution of $[Et_4N][TpMo(CO)_3]$ (9.97 g, 19.1 mmol) and Cp_2FePF_6 (5.59 g, 19.1 mmol) in 150 mL of acetonitrile was refluxed until gas (CO) evolution ceased and the color of the mixture had turned to a green-brown. The solvent was removed under reduced pressure, and the Cp_2Fe was sublimed under vacuum out of the solid residue onto a cold finger. Hot $CHCl_3$ (100 mL) was added to the resulting residue, and the deep green solution was filtered. Concentration of the filtrate to a volume of 10 mL gave green crystals which were washed with 10 mL of cold $CHCl_3$ and dried under vacuum to give 5.70 g of air-stable product, mp 193–195 °C. The average yield of several preparations was 72%. The product so obtained was shown by a single-crystal X-ray structure determination and by analysis to be the solvate, $Tp_2Mo_2(CO)_4 \cdot CHCl_3$: IR (KBr) 1966 (s), 1897 (s), 1849 (s), 1837 (s) cm^{-1}; IR (PhMe soln) 1970 (s), 1905 (s), 1856 (s), 1842 (s) cm^{-1}; ^1H NMR ($CDCl_3$) 8.30 d(A), 8.38 d(B) [H_3, 6 H], 7.48 d(A), 7.63 d(B) [H_5, 6H], 7.30 d(A), 7.34 d(B) [H_4, 6 H], A:B = 1:2; $^3J_{H_3,H_4}$ = 1.9 Hz, $^3J_{H_5,H_4}$ = 1.7 Hz; $^{13}C\{^1H\}$ ($CDCl_3$, 90.56 MHz) 147 (A), 142 (B) [C_3], 134 (A), 135 (B) [C_5], 107 (A), 105 (B) [C_4], 232 and 239, CO, A:B = 1:2. Anal. Calcd for $C_{23}H_{19}B_2Cl_3Mo_2N_{12}O_4$ ($Tp_2Mo_2(CO)_4 \cdot CHCl_3$): C, 32.52; H, 2.49. Found: C, 32.30; H, 2.42.

Darker green, unsolvated crystals may be obtained by adding toluene instead of $CHCl_3$ to the residue from the sublimation in the above procedure. Heating the chloroform–solvate (80–100 °C) under vacuum for several hours also removes the $CHCl_3$ from the solvate. The unsolvated compound melts at 200 °C with decomposition. $Tp_2Mo_2(CO)_4$ may also be obtained from isolated **1**. Thermolysis of **1** (3.0 g, 7.6 mmol) in refluxing diglyme for 10 min gave 2.71 g (97%) of **2**. Acetonitrile may be substituted for the diglyme, but the reaction time is increased.

Reaction of 1 with $Cp_2Mo_2(CO)_n$ (n = 4, 6). A toluene solution (50 mL) of **1** (0.50 g, 1.27 mmol) and $Cp_2Mo_2(CO)_4$ (0.55 g, 1.27 mmol) was refluxed for 2 h. The toluene was pumped off under vacuum, and the residue was taken up in C_6D_6. ^1H NMR spectra revealed only starting materials to be present. A similar reaction in which 0.80 g (2.0 mmol) of **1** and 0.50 g (1.0 mmol) of $Cp_2Mo_2(CO)_6$ in 200 mL of toluene was refluxed for 2 h gave a mixture containing $Cp_2Mo_2(CO)_4$, $Cp_2Mo_2(CO)_6$, and **1** as determined by IR. Continuing the reflux period for an additional 12 h caused a color change from red-brown to dark brown. A solution IR showed a high concentration of $Cp_2Mo_2(CO)_4$, along with $Cp_2Mo_2(CO)_6$ and **1** at about $^1/_4$ of their initial concentrations.

(1) Reactions of 2 with CO. Compound **2** and CO (1 atm) failed to react, even in refluxing toluene. However, **2** (0.21 g, 0.29 mmol) in 40 mL of toluene reacted under 2500 psi of CO at 35 °C for 3 days gave a yellow-brown solution. Removal of the toluene under vacuum gave 0.07 g (45%) of $Mo(CO)_6$ upon sublimation of the residue. The solid remaining from the sublimation did not exhibit ν_{CO} bands in the IR and was not further characterized.

(2) With Na. Excess Na foil was added to a solution of **2** (0.24 g, 0.33 mmol) in 20 mL of THF. The color changed from green to yellow brown, and after 1 h, an IR spectrum showed the absence of **2** and the presence of $Na[TpMo(CO)_3]$ and minor amounts of other carbonyl containing species (ν_{CO} 2030 (s), 1805 (s), and 1710 (s) cm^{-1}). Excess CH_3I was added, and the solution was refluxed for 18 h. An IR spectrum then showed the presence of $TpMo(CO)_2(\eta^2\text{-}COMe)$,[5b,7] the expected product from the reaction of $TpMo(CO)_3^-$ and CH_3I, and the minor carbonyl bands had shifted to 1937 (s), 1858 (s), and 1710 (s) cm^{-1}.

(3) With I_2. Iodine (0.10 g, 0.40 mmol) was added to **2** (0.27 g, 0.37 mmol) dissolved in 15 mL of toluene, and the solution was stirred for 0.5 h. An IR spectrum showed only partial conversion of **2**, so an additional 0.10 g of I_2 was added. An IR spectrum, recorded after 4 min, showed complete conversion of **2**. The solvent was removed under vacuum, and the residue was washed with 10 mL of CH_3CN. The solid (0.13 g, 33%) was identical with authentic $TpMo(CO)_3I$.[5a]

(4) With Br_2. Bromine (0.20 g, 1.25 mmol) in 10 mL of CH_2Cl_2 was added to **2** (0.20 g, 0.27 mmol) in 10 mL of CH_2Cl_2, and the mixture was stirred for 10 min to give complete conversion of **2**. The volume of the solution was reduced to ca. 7 mL, and 20 mL of CH_3OH was added to give a dark yellow solid (0.08 g, 31%) shown to be $TpMo(CO)_3Br$ by comparison with an authentic sample.[5]

(5) With Other Reagents. No reaction was observed between **2** and propylene sulfide, S_8, PhC≡CH, EtC≡CH, or $P(OMe)_3$ under prolonged refluxing toluene. Likewise, no reaction was observed with H_2 (3500 psi) at 35 °C after 1 day. Ph_2CN_2 or Cp_2FePF_6 did not react with

(5) (a) Curtis, M. D.; Shiu, K.-B. *Inorg. Chem.* **1985**, *24*, 1213. (b) Curtis, M. D.; Shiu, K.-B.; Butler, W. M. *J. Am. Chem. Soc.* **1986**, *108*, 1550.

(6) Trofimenko, S. *Acc. Chem. Res.* **1971**, *9*, 17. Trofimenko, S. *Chem. Rev.* **1972**, *72*, 487.

(7) Shiu, K.-B.; Curtis, M. D. *Organometallics* **1983**, *2*, 1475.

(8) (a) Collins, D. M.; Cotton, F. A.; Murillo, C. A. *Inorg. Chem.* **1976**, *15*, 1861. (b) Louie, B. M.; Rettig, S. J.; Storr, A.; Trotter, J. *Can. J. Chem.* **1984**, *62*, 633. (c) Cocivera, M.; Desmond, T. J.; Ferguson, G.; Kaitner, B.; Lalor, F. J.; O'Sullivan, D. J. *Organometallics* **1982**, *1*, 1125.

(9) Shiu, K.-B.; Curtis, M. D.; Huffman, J. C. *Organometallics* **1983**, *2*, 936.

(10) Beck, W.; Schleter, K. *Z. Naturforsch. B: Anorg. Chem., Org. Chem.* **1978**, *33B*, 1214.

(11) Curtis, M. D.; Fotinos, N. A.; Messerle, L.; Sattelberger, A. P. *Inorg. Chem.* **1983**, *22*, 1559.

(12) Smart, J. C.; Dinsky, B. L. *J. Am. Chem. Soc.* **1980**, *102*, 1009.

(13) Adams, R. D.; Collins, D. M.; Cotton, F. A. *Inrog. Chem.* **1974**, *13*, 1086.

Table I. Crystal Data for $TpMo(CO)_3$ and $Tp_2Mo_2(CO)_4 \cdot CHCl_3$

	$TpMo(CO)_3$	$Tp_2Mo_2(CO)_4 \cdot CHCl_3$
fw (g/mol)	392.8	849.36
color	red-brown	green
ρ_{calcd} (g cm^{-3})	1.43	1.74
radiatn	Mo Kα	Mo Kα (λ = 0.71069)
2θ max (deg)	45	50
a	11.359 (4)	12.995 (2)
b	11.359 (4)	16.974 (4)
c	8.161 (2)	29.396 (6)
α, β (deg)	90.0	90.0
γ (deg)	120.0	90.0
V(Å^3), Z	911.9 (3), 2	6485 (2), 8
space group	$P\bar{3}$ (no. 147)	$Pbca$ (no. 61)
cryst dimens (mm)	0.20 × 0.20 × 0.20	0.16 × 0.20 × 0.22
μ(cm^{-1})	14.31	10.54
I_{max}, I_{min}[a]	0.75, 0.75	0.84, 0.79
N, NO, NV[b]	501, 448*, 96	6796, 2957, 315
R_1, R_2	0.038, 0.043	0.055, 0.063
GOF[c]	2.40	1.71

[a] Calculated maximum and minimum transmitted intensities. [b] N = independent reflections, NO = number with $I > 2.33\sigma(I)$(*) or $I > 3\sigma(I)$, NV = number of variables. [c] Goodness of fit = $[w(|F_o| - |F_c|)^2/(NO - NV)]^{1/2}$.

2 in refluxing CH_2Cl_2. HCl gas and **2** in MeCN reacted at room temperature to give a complex mixture (no ν_{CO}) from which no pure compounds were isolated.

Reaction of 1 with S_8 or Propylene Sulfide. Elemental sulfur (0.08 g, 2.5 mmol) or propylene sulfide (0.3 mL, 3 mmol) was added to **1** (1.0 g, 2.5 mmol) in 50 mL of CH_2Cl_2. Immediate gas evolution was noted, and after 6 min, the color of the solution had changed from red-brown to dark green. Ethanol (30 mL) was added, and the CH_2Cl_2 was pumped off under reduced pressure. A blue-green solid (0.77 g, 80%) crystallized and was characterized as $[TpMo(CO)_2]S$:[14] MS, P^+, $(P - 2CO)^+$, $(P - 3CO)^+$, $(P - 4CO)^+$ (P = parent ion); IR (KBr) 1990 (s), 1930 (s), 1890 (s), 1860 (s) cm^{-1}; IR (CH_2Cl_2) 2000 (s), 1947 (s), 1925 (s), 1892 (sh) cm^{-1}; ^{1}H NMR ($CDCl_3$) 7.85 d(B), 7.55 d(A) [H_3, 6 H], 7.68 d(B), 7.43 d(A) [H_5, 6 H], 6.24 t(B), 6.05 t(A) [H_4, 6 H], A:B = 1:2, $^3J_{H_3,H_4}$ = 2.3 Hz, $^3J_{H_4,H_5}$ = 1.8 Hz; mp 278–281 dec. Anal. Calcd for $C_{22}H_{20}B_2Mo_2N_{12}O_4S$: C, 34.68; H, 2.65. Found: C, 35.69; H, 2.69.

X-ray Structure of 1. Crystals of **1** were grown from CH_2Cl_2/hexane at room temperature. These crystals had two distinct habits consisting of hexagonal or star-shaped plates and a darker rhombic form. Crystals of both habits were shown to have identical cell parameters. A nearly equidimensional crystal of the second form was selected for the structure determination and mounted on a glass fiber with silicone grease in a N_2-filled bag. The goniometer was then transferred into the cold N_2 stream of the cooling system on the diffractometer.

A systematic search of a limited hemisphere of reciprocal space revealed a trigonal lattice with no extinctions. The structure refined successfully in space group $P\bar{3}$ (No. 147). Diffraction data were collected at −169 ± 4 °C, and the structure was solved by a combination of direct methods (Multan 78) and Fourier syntheses. ψ scans of 6 reflections indicated that no absorption correction was necessary (max variation, 5%). All atoms with the exception of the H atom on B were located and refined. The final difference Fourier was essentially featureless. Crystal and data statistics are given in Table I, and the atomic coordinates are in Table II. Thermal parameters are in Table III (supplementary material), and bond distances and angles are listed in Table IV.

X-ray Structure of 2. Crystals of **2** were grown from $CHCl_3$/hexane at room temperature and mounted on a Syntex $P2_1$ diffractometer. Initial rotation photos indicated the orthorhombic system. Cell dimensions were obtained from 15 refined reflections dispersed in reciprocal space, and a search of a limited hemisphere indicated the space group to be *Pbca* (No. 61). Crystal and data collection statistics are presented in Table I. The positions of the Mo atoms were determined from a Patterson map and the remaining atomic positions from subsequent difference maps. The final difference map showed peaks (0.5–1.2 e/Å^3) in positions reasonable for H atoms, but these were ignored. The fractional atomic coordinates are listed in Table VI, the thermal parameters in Table VII (supplementary material), and selected bond lengths and angles in Table VIII. Table IX lists least-squares planes and Table X the F_o vs. F_c (supplementary material).

Table II. Fractional Coordinates and Isotropic Thermal Parameters for $TpMo(CO)_3$[a,b]

atom	x	y	z	B_{iso}
Mo	6667*	3333*	2759 (2)	10
B	6667*	3333*	−1316 (23)	10
N_{12}	7908 (7)	4637 (7)	−642 (8)	8
N_{11}	8135 (7)	4822 (7)	1004 (8)	11
C_{11}	9298 (10)	6001 (9)	1166 (13)	14
C_{13}	3218 (10)	−203 (10)	323 (12)	16
C_{12}	8895 (10)	5685 (10)	−1421 (12)	14
C_1	5256 (11)	1907 (11)	4237 (11)	24
O_1	4466 (10)	1146 (9)	5096 (9)	50
H_{11}	948 (8)	624 (8)	207 (9)	0 (19)
H_{13}	300 (8)	31 (9)	60 (9)	0 (19)
H_{12}	891 (8)	574 (7)	−248 (9)	0 (16)

[a] Fractional coordinates are ×10^4 for non-hydrogen atoms and ×10^3 for hydrogen atoms. B_{iso} values are ×10. [b] Parameters marked by an asterisk, *, were not varied.

Results and Discussion

$TpMo(CO)_3$ (1). Synthesis. One-electron oxidation of the anion, $TpMo(CO)_3^-$, with mild oxidizing agents, e.g., Cp_2Fe^+, Ag^+, Ph_3C^+, etc., gives the paramagnetic radical, **1**, according to eq 1. Highest yields and easiest workup of **1** are obtained with Cp_2FePF_6 as the oxidant.

$$TpMo(CO)_3^- + Ox \rightarrow TpMo(CO)_3 + Red \quad (1)$$

Compound **1** is a red-brown solid which exhibits ν_{CO} bands at 2010 and 1885 cm^{-1}. These frequencies are 110–120 cm^{-1} higher than the ν_{CO} of the anion, $TpMo(CO)_3^-$, indicative of decrease Mo–CO π-bonding in the neutral species.

The radical decomposes slowly (weeks) under N_2 at 25 °C. In a sealed capillary, the compound darkens at 170 °C and melts with decomposition at 189 °C. This thermal stability contrasts sharply with that of $CpMo(CO)_3$, which although in equilibrium with the dimer, $Cp_2Mo_2(CO)_6$, in solution at temperatures >100 °C can only be isolated in a low-temperature matrix.[16] The increased thermal stability of **1** relative to $CpMo(CO)_3$ is due to the pronounced prospensity of the TpMo fragment to assume an octahedral geometry by coordination of only three ligands as opposed to the commonly observed seven-coordinate $CpMoL_4$ structures.[5] Thus, the six-coordinate radical **1** shows little tendency to dimerize and become seven-coordinate through formation of a metal–metal bond.

The steric bulk of the Tp ligand undoubtedly discourages high coordination numbers. The cone angle of the Tp ligand is nearly 180° (see Figure 2). Interleaving additional ligands between the pyrazolyl rings leads to the preferred octahedral coordination. It has also been suggested[5] that the donor orbitals on the Tp ligand, localized on the N atoms, are more effective in hybridizing the metal fragment orbitals into an octahedral array than the diffuse, π-donor orbitals of Cp. Thus, both steric and electronic effects promote six-coordination in the Tp complexes as compared to their Cp analogues. In order to interpret the ^{1}H NMR of **1** (see below), and in order to compare the bonding of Tp and Cp ligands to a common metal fragment, an EHMO calculation of $TpMo(CO)_3$ was undertaken. These results are presented next.

EHMO Calculation. The Mo's of the Tp ligand are constructed from the MO's of the constituent pyrazole rings. The relevant MO's of pyrazole are shown in Figure 1A and Scheme I. There are three π-MO's, $\pi_{1\pm}$ and π_{2-}, labeled according to the number of nodes and according to whether a node bisects the N–N bond (−) or does not (+), which are important in the makeup of the Tp^- ligand. Two other orbitals, π_0 (lowest E) and π_{2+} (highest E), do not interact strongly with the $Mo(CO)_3$ fragment and are omitted from Figure 1. The π_0, $\pi_{1\pm}$, and $\pi_{2\pm}$ orbitals resemble the familiar a_1, e', e'' orbitals of Cp^- (Scheme I). In addition to the π-orbitals, the "lone pairs", σ_N, are MO's which have large

(14) Lincoln, S.; Soong, S.-L.; Koch, S. A.; Sato, M.; Enemark, J. H. *Inorg. Chem.* **1985**, *24*, 1355.

(15) Curtis, M. D.; Klingler, R. J. *J. Organomet. Chem.* **1978**, *161*, 23.
(16) Mahmoud, K. A.; Rest, A. J. *J. Organomet. Chem.* **1983**, *246*, C37.

Table IV. Bond Distances (A) and Angles (deg) for $TpMo(CO)_3$

$Mo-N_{11}$	2.207 (7)	$Mo-C_1$	2.013 (11)	C_1-O_1	1.126 (11)
$N_{11}-N_{12}$	1.365 (9)	$N_{12}-C_{12}$	1.320 (11)	$C_{12}-C_{13}$	1.359 (13)
$C_{13}-C_{11}$	1.363 (15)	$C_{11}-N_{11}$	1.337 (11)	$N_{12}-B$	1.548 (10)

$N_{11}-Mo-N'_{11}$	82.5 (3)	$N_{11}-Mo-C_1$	94.8 (3)
$N_{11}-N_{12}$	120.6 (9)	$N_{11}-N_{12}-C_{12}$	109.0 (7)
$C_1-Mo-C'_1$	87.8 (4)	$C_{12}-N_{12}-B'$	130.4 (9)
$C_{12}-C_{13}-C_{11}$	104.5 (10)	$Mo-N_{11}-N_{12}$	120.6 (5)
$Mo-N_{11}-C_{11}$	133.9 (7)	$N_{12}-N_{11}-C_{11}$	105.5 (7)
$N_{11}-C_{11}-C_{13}$	111.1 (9)	$N_{12}-C_{12}-C_{13}$	109.9 (8)
$Mo-C_1-O_1$	177.5 (8)	$N_{12}-B-N'_{12}$	108.1 (8)

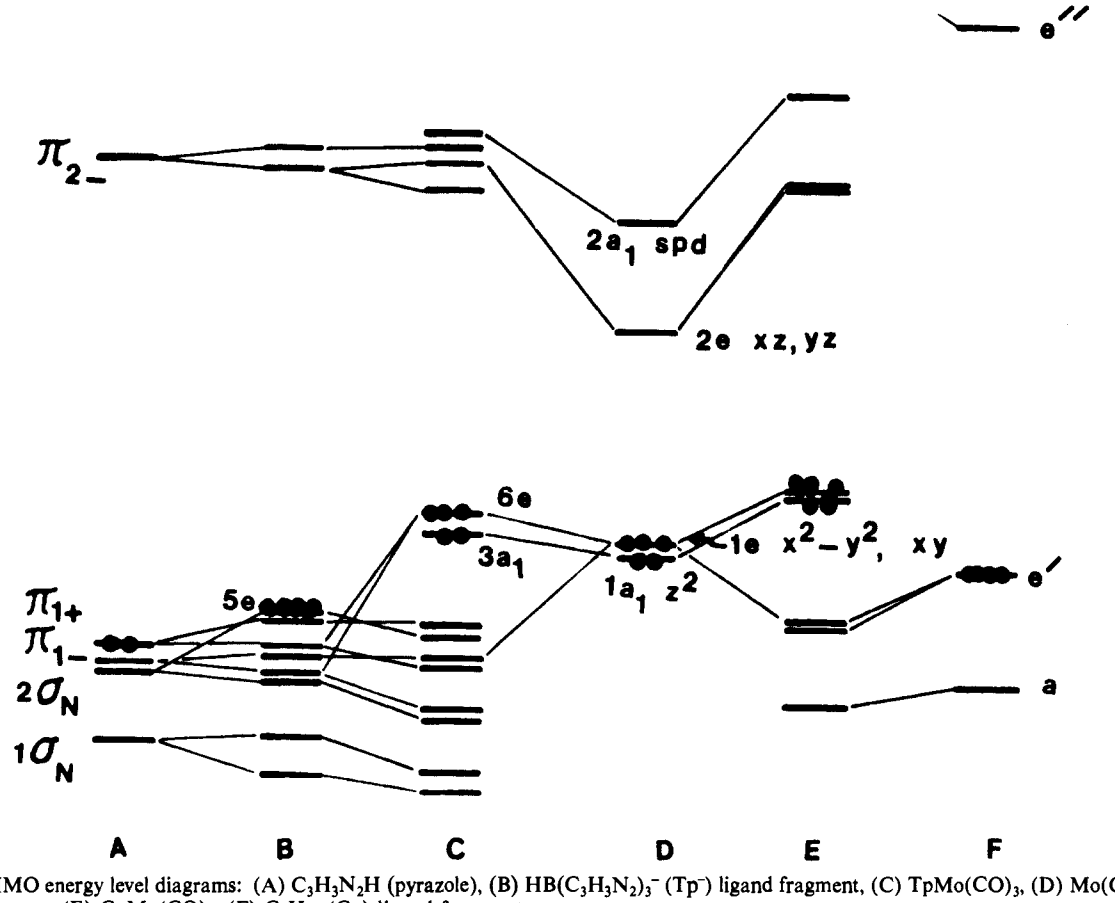

Figure 1. EHMO energy level diagrams: (A) $C_3H_3N_2H$ (pyrazole), (B) $HB(C_3H_3N_2)_3^-$ (Tp^-) ligand fragment, (C) $TpMo(CO)_3$, (D) $Mo(CO)_3^+$ metal carbonyl fragment, (E) $CpMo(CO)_3$, (F) $C_5H_5^-$ (Cp) ligand fragment.

Scheme I

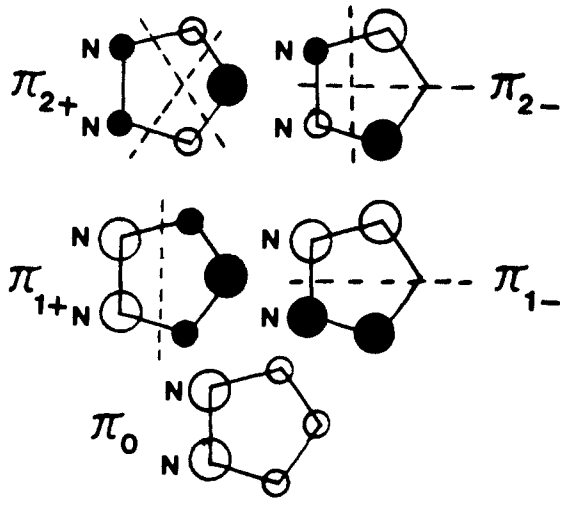

coefficients on the terminal nitrogens (N-2) of the pyrazole rings. There are *two* such σ_N orbitals which interact strongly with the $Mo(CO)_3$ fragment (i.e., the "lone pair" character is shared by two MO's labeled $1\sigma_N$ and $2\sigma_N$).

Scheme II

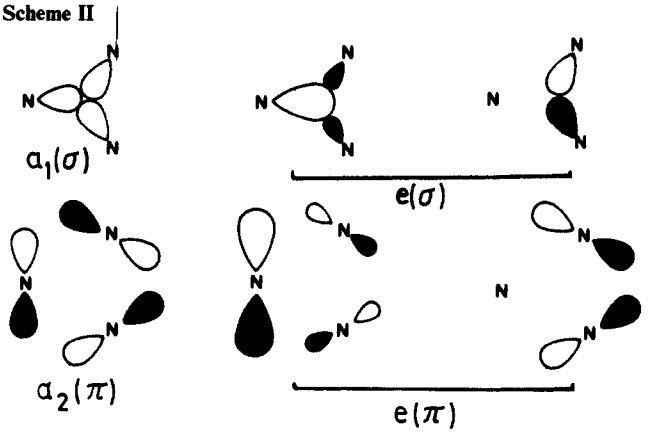

When the three pyrazole rings are assembled into a Tp^- anion of C_{3v} symmetry, the lone pair (σ_N) orbitals form the $a_1 + e$ combinations shown in Scheme II. Each of the π-type MO's form $a_2 + e$ sets, also shown in Scheme II. The energies of the pyrazole ring orbitals are perturbed by the close proximity of the neighboring rings in the Tp ligand and form the energy levels as shown

Table VI. Fractional Atomic Coordinates for $Tp_2Mo_2(CO)_4 \cdot CHCl_3$

atom	x	y	z
Mo_1	0.4872 (1)	0.2000 (1)	0.64822 (3)
Mo_2	0.5820 (1)	0.0773 (1)	0.62607 (3)
C	0.368 (1)	−0.3572 (9)	0.6006 (5)
Cl_1	0.3276 (4)	−0.2640 (3)	0.5892 (2)
Cl_2	0.476 (1)	−0.3549 (3)	0.6344 (2)
Cl_3	0.394 (1)	−0.4073 (3)	0.5519 (2)
C_{21}	0.625 (1)	0.1617 (7)	0.5859 (4)
C_{22}	0.691 (1)	0.1214 (7)	0.6649 (4)
N_{211}	0.486 (1)	0.0075 (5)	0.5780 (3)
N_{221}	0.565 (1)	−0.0321 (5)	0.6670 (3)
N_{231}	0.706 (1)	0.0092 (5)	0.5925 (3)
C_{11}	0.396 (1)	0.1109 (7)	0.6484 (4)
C_{12}	0.515 (1)	0.1632 (7)	0.7101 (4)
N_{111}	0.354 (1)	0.2616 (5)	0.6780 (3)
N_{121}	0.436 (1)	0.2649 (5)	0.5858 (3)
N_{131}	0.563 (1)	0.3155 (5)	0.6600 (3)
O_{21}	0.663 (1)	0.2063 (5)	0.5613 (3)
O_{22}	0.756 (1)	0.1454 (6)	0.6844 (3)
C_{211}	0.406 (1)	0.0267 (8)	0.5503 (4)
N_{212}	0.506 (1)	−0.0698 (5)	0.5709 (3)
C_{221}	0.554 (1)	−0.0459 (8)	0.7124 (4)
N_{222}	0.576 (1)	−0.1041 (5)	0.6477 (4)
C_{231}	0.801 (1)	0.0304 (7)	0.5773 (4)
N_{232}	0.695 (1)	−0.0695 (6)	0.5844 (3)
O_{11}	0.332 (1)	0.0630 (5)	0.6529 (3)
O_{12}	0.542 (1)	0.1441 (5)	0.7473 (3)
C_{111}	0.278 (1)	0.2361 (8)	0.7044 (4)
N_{112}	0.332 (1)	0.3380 (6)	0.6661 (3)
C_{121}	0.426 (1)	0.2424 (7)	0.5414 (4)
N_{122}	0.405 (1)	0.3406 (6)	0.5883 (4)
C_{131}	0.657 (1)	0.3341 (8)	0.6779 (4)
N_{132}	0.512 (1)	0.3845 (5)	0.6537 (3)
C_{213}	0.374 (1)	−0.0399 (9)	0.5256 (4)
C_{223}	0.557 (1)	−0.1264 (8)	0.7209 (5)
C_{233}	0.851 (1)	−0.0353 (9)	0.5594 (4)
C_{113}	0.203 (1)	0.2960 (9)	0.7103 (5)
C_{123}	0.384 (1)	0.3070 (9)	0.5164 (5)
C_{133}	0.663 (1)	0.4171 (8)	0.6846 (4)
C_{212}	0.441 (1)	−0.0995 (8)	0.5392 (4)
C_{222}	0.571 (1)	−0.1625 (7)	0.6786 (4)
C_{232}	0.780 (1)	−0.0962 (7)	0.5633 (4)
C_{112}	0.212 (1)	0.3605 (8)	0.6863 (4)
C_{122}	0.373 (1)	0.3654 (8)	0.5471 (5)
C_{132}	0.568 (1)	0.4458 (7)	0.6700 (4)
B_2	0.593 (1)	−0.1126 (9)	0.5944 (5)
B_1	0.401 (1)	0.3842 (8)	0.6346 (5)

in Figure 1B. The 5e orbital is the HOMO and is derived from the N "lone pair" orbitals.

The relevant orbitals of the $Mo(CO)_3$ fragment, shown in Figure 1D, are the $1a_1(z^2)$, $1e(x^2 - y^2, xy)$, $2e(xz, yz)$, and a hybrid, $2a_1(sp_z z^2)$. The σ_N a_1 orbitals have poor overlap with the z^2 orbital on the $Mo(CO)_3^+$ fragment. Consequently, the $1a_1(z^2)$ orbital is pushed up only slightly in energy. The overlap integral of the $2a_1$(spd) hybrid with the σ_N orbitals of Tp^- is larger ($S \approx 0.1$), and the spd hybrid is destabilized considerably. The $1e(x^2 - y^2, xy)$ orbital of the $Mo(CO)_3$ fragment interacts primarily with both the $3e(\pi_{1-})$ and $4e(\pi_{1+})$ combinations of the Tp fragment to form the HOMO, 6e, of the $TpMo(CO)_3$ molecule. The $3e(xz, yz)$ orbital of the $Mo(CO)_3$ fragment overlaps strongly with both $2e(\sigma)$ and $3e(\pi_{1-})$ and is pushed up to high energy. The HOMO LUMO gap is ca. 3 eV.

Comparison of Tp and Cp. Since the Tp ligand is often compared to Cp, it is interesting to compare the bonding of these two ligands to a common metal fragment. The energy levels of Cp^- and $CpMo(CO)_3$ are shown in the right side of Figure 1. The energy levels of $TpMo(CO)_3$ and $CpMo(CO)_3$ are very similar. However, the makeup of the orbitals in these two compounds in considerably different as shown by a fragment molecular orbital (FMO) population analysis.

In the FMO population analysis, the molecular orbitals are expressed as linear combinations of the FMO's. The population of each FMO, summed over all occupied MO's, is computed. These reduced FMO populations are shown in Table XI. For

Table VIII. Bond Distances (Å) and Bond Angles (deg) for $Tp_2Mo_2(CO)_4 \cdot CHCl_3$

bonds	$n = 1$	$n = 2$	$n = 3$	av
Mo_1–C_{1n}	1.92 (1)	1.96 (1)		1.95 ± 0.02
Mo_2–C_{2n}	1.94 (1)	1.97 (1)		
Mo_1–N_{1n1}	2.206 (9)	2.243 (9)	2.221 (9)	2.222 ± 0.008
Mo_2–N_{2n1}	2.225 (9)	2.222 (9)	2.216 (9)	
N_{1n1}–N_{1n2}	1.37 (1)	1.35 (1e	1.36 (1e	1.36 ± 0.01
N_{2n1}–N_{2n2}	1.35 (1)	1.35 (1)	1.36 (1)	
N_{1n1}–C_{1n1}	1.34 (1)	1.37 (1)	1.37 (1)	1.36 ± 0.01
N_{2n1}–C_{2n1}	1.36 (1)	1.36 (1)	1.36 (1)	
C_{1n1}–C_{1n3}	1.40 (2)	1.43 (2)	1.42 (2)	1.41 ± 0.01
C_{2n1}–C_{2n3}	1.41 (2)	1.39 (2)	1.40 (2)	
C_{1n3}–C_{1n2}	1.39 (2)	1.35 (2)	1.39 (2)	1.38 ± 0.01
C_{2n3}–C_{2n2}	1.39 (2)	1.40 (2)	1.39 (2)	
C_{1n2}–N_{1n2}	1.37 (1)	1.35 (1)	1.36 (1)	1.35 ± 0.01
C_{2n_2}–N_{2n2}	1.35 (1)	1.35 (1)	1.35 (1)	
B–N_{1n2}	1.50 (2)	1.55 (2)	1.55 (2)	1.54 ± 0.02
B–N_{2n2}	1.52 (2)	1.59 (2)	1.54 (2)	
C_{1n}–O_{1n}	1.18 (1)	1.15 (1)		1.16 ± 0.01
C_{2n}–O_{2n}	1.16 (1)	1.14 (1)		
Mo_1–Mo_2	2.507 (1)			
C–Cl_n	1.70 (2)	1.72 (1)	1.70 (2)	1.70 ± 0.01

Angles

C_{11}–Mo_1–C_{12}	81.9 (5)	C_{11}–Mo_1–N_{111}	83.6 (4)
C_{11}–Mo_1–N_{121}	101.8 (4)	C_{11}–Mo_1–N_{131}	165.6 (4)
C_{12}–Mo_1–N_{111}	85.8 (4)	C_{12}–Mo_1–N_{121}	166.5 (4)
C_{12}–Mo_1–N_{131}	93.2 (4)	N_{111}–Mo_1–N_{121}	81.8 (4)
N_{111}–Mo_1–N_{131}	82.5 (3)	N_{121}–Mo_1–N_{131}	80.0 (4)
C_{11}–Mo_1–Mo_2	69.4 (3)	C_{12}–Mo_1–Mo_2	83.4 (3)
Mo_1–C_{11}–O_{11}	170.0 (1)	Mo_1–C_{12}–O_{12}	175.0 (1)
Mo_1–N_{111}–N_{112}	120.4 (7)	Mo_1–N_{121}–N_{122}	120.8 (7)
Mo_1–N_{131}–N_{132}	121.5 (7)	Mo_1–N_{111}–C_{111}	131.7 (8)
Mo_1–N_{121}–C_{121}	132.2 (8)	Mo_1–N_{131}–C_{131}	131.3 (8)
N_{211}–Mo_2–Mo_1	109.5 (2)	N_{111}–Mo_1–Mo_2	152.1 (2)
N_{231}–Mo_2–Mo_1	155.1 (3)	N_{131}–Mo_1–Mo_2	123.8 (2)
N_{221}–Mo_2–Mo_2	120.4 (2)	N_{121}–Mo_1–Mo_2	110.1 (2)
C_{21}–Mo_2–C_{22}	82.2 (5)	C_{21}–Mo_2–N_{211}	99.6 (4)
C_{21}–Mo_2–N_{221}	167.2 (4)	C_{21}–Mo_2–N_{231}	84.5 (4)
C_{22}–Mo_2–N_{211}	166.9 (4)	C_{22}–Mo_2–N_{221}	94.3 (4)
C_{22}–Mo_2–N_{231}	86.2 (4)	N_{211}–Mo_2–N_{221}	81.0 (3)
N_{211}–Mo_2–N_{231}	81.1 (3)	N_{221}–Mo_2–N_{231}	82.9 (3)
C_{21}–Mo_2–Mo_1	71.6 (3)	C_{22}–Mo_2–Mo_1	83.5 (3)
Mo_2–C_{21}–O_{21}	171.0 (1)	Mo_2–C_{22}–O_{22}	174.0 (1)
Mo_2–N_{211}–N_{212}	120.7 (7)	Mo_2–N_{221}–N_{222}	121.2 (7)
Mo_2–N_{231}–N_{232}	12.07 (7)	Mo_2–N_{211}–C_{211}	132.8 (8)
Mo_2–N_{221}–C_{221}	133.1 (8)	Mo_2–N_{231}–C_{231}	131.9 (8)

Average Values[a]

N_t–C–C	110 [1]	N_B–B–N_B	108 [2]
N_B–C–C	109 [2]	N_t–N_B–B	121 [1]
N_t–N_B–C	110 [1]	C–N_B–B	128 [1]
N_B–N_t–C	107 [1]	C–C–C	105 [1]

[a] Standard deviations in square brackets calculated by $\sigma = (\sum(x - \bar{x})^2/(n-1))^{1/2}$; $N_t = N_{nm1}$, $N_B = N_{nm2}$ ($n = 1, 2$; $m = 1, 2, 3$).

Table XI. Fragment Molecular Orbital (FMO) Populations in $TpMo(CO)_3$ and $CpMo(CO)_3$

	pop.	Δ[a]	$Mo(CO)_3^+$ FMO	pop.	Δ
		$TpMo(CO)_3$			
Tp^- FMO					
$6e(\pi)$	0.04	+0.04	$2a_1$(spd)	0.14	+0.14
$5e(\sigma)$	3.73	−0.27	$2e(xz, yz)$	0.73	+0.73
$4e(\pi)$	3.88	−0.12	$1e(x^2 - y^2, xy)$	3.07	+0.07
$3e(\pi)$	3.73	−0.27	$1a_1(z^2)$	2.00	0.0
$2e(\sigma)$	3.87	−0.13			
$2a_1(\sigma)$	1.85	−0.15			
$1a_1(\sigma)$	1.94	−0.06			
		$CpMo(CO)_3$			
Cp^- FMO					
e″	0.08	+0.08	$2a_1$	0.04	+0.04
e′	3.29	−0.71	2e	0.66	+0.66
a_1	1.90	−0.10	1e	2.96	−0.04
			$1a_1$	1.99	−0.01

[a] Δ is the electron loss (−) or gain (+) experienced by the FMO's upon molecule formation.

Table XII. Calculated Contact Hyperfine Coupling Constants[a] and ^{1}H NMR Paramagnetic Shifts[b] in $TpMo(CO)_3$ due to σ- and π-Delocalization

proton	$A(\sigma) \times 10^2$	$A(\pi)$	$\Delta\delta(\sigma)$	$\Delta\delta(\pi)$	$\Delta\delta$(net)	$\Delta\delta$(obsd)
H_5	1.35	−0.36	−1.81	+26.8	25.0	25.8
H_4	0.36	−0.13	−0.27	+9.8	9.5	3.1
H_3	2.44	−0.22	−1.00	+16.2	15.2	15.7

[a] In G. [b] In ppm.

example, the population of the Cp(1e′) FMO in $CpMo(CO)_3$ is 3.29 electrons. These Cp orbitals contained 4.0 electrons in the free Cp^- ion, so that 0.71 electron is transferred out of the Cp(1e′) orbitals upon bonding Cp^- to the $Mo(CO)_3^+$ fragment.

In $TpMo(CO)_3$ there are several important interactions as shown by the FMO populations in Table XI. The FMO's derived from nitrogen "lone pairs" (5e, 2e, $2a_1$) all show significant population decreases compared to their values in free Tp^- as do the 4e and 3e FMO's derived from the π_{1+} and π_{1-} orbitals of the pyrazole rings. There is a total of 1.0 electron donated to the $Mo(CO)_3^+$ fragment, compared to 0.81 electron donated by Cp. Thus, Tp^- is a better donor than Cp^-. The (xz, yz) orbitals, which have π-symmetry with respect to the principal axis, are the accepted orbitals on the metal. Therefore, both Tp^- and Cp^- are good π-donors. Neither is a good π-acceptor. It is interesting to note that the Tp ligand forms strong π-bonds to the metal with its *σ-donor* orbitals.

^{1}H NMR of 1. One of the reasons for performing the EHMO calculations was to aid the interpretation of the ^{1}H NMR spectrum of **1**. This spectrum consists of three broadened singlets shifted upfield from their positions in diamagnetic compounds. In C_6D_6 and $CDCl_3$, the average chemical shifts are δ 3.1, −8.5, and −18.8. In acetone-d_6, the shifts are δ 3.52, −7.69, and −17.11. These differences suggest that acetone may be weakly coordinated to the paramagnetic complex.

Paramagnetic shifts in the NMR spectrum are caused by perturbations of the magnetic field at a proton by fields associated with the unpaired electron.[17,18] One contribution to the paramagnetic shift is the Fermi contact term, given by

$$\frac{\Delta H}{H} = \frac{-Ag^2\beta^2 S(S+1)}{3g_N\beta_N kT} \quad (A \text{ in G})$$

or

$$\Delta\delta = (\Delta H/H) \times 10^6 = -74.1A \text{ for } T = 298\ ^\circ\text{C},\ S = \tfrac{1}{2}$$

where A = isotropic hyperfine coupling constant.

The hyperfine coupling constant has contributions from directly delocalized spin density and from spin polarization. The EHMO calculation allows us to separate these two contributions as follows. The odd electron is in the doubly degenerate HOMO, 6e, viewed down the C_3 axis in Scheme III.

The $x^2 - y^2$ component is strictly σ-bonding with respect to the pyrazolyl ring in the yz plane, and the xy component is strictly π-bonding to this ring. The other two rings experience both σ- and π-components, but the combined effect is the same for all rings because they are symmetry equivalent. On the average, one-half of the odd electron is in $x^2 - y^2$ and one-half in xy. The $x^2 - y^2$ can only mix with σ-donor orbitals on the (yz) ring, and the odd electron is directly delocalized onto the ring protons. The hyperfine coupling constant due to this direct σ-delocalization is $A_\sigma = (^1/_2)C_{\sigma i}^2(507)$. Here, 507 is the hyperfine constant of the hydrogen atom, and $C_{\sigma i}^2$ is the square of the coefficient of the ith H atom in the predominantly $x^2 - y^2$ MO. The factor $^1/_2$ accounts for the fact that only one-half of an odd electron is in the $x^2 - y^2$ MO. The constants, A_σ, so calculated are shown in Table XII.

Conversely, the unpaired electron in the xy orbital is delocalized onto the ring exclusively by π-bonding. In this case, the ring H atoms lie in the nodal plane and experience no *directly* delocalized spin density. This situation is analogous to that of planar, aromatic radical anions in which the proton hyperfine coupling constant, A_π, caused by spin polarization from the π-system is given by the McConnell equation, $A_\pi = -Q_\pi\rho_c$. Here, ρ_c is the spin density in the p_π orbital of the carbon atom to which the proton is bonded and Q_π is a constant.[19] A value of 28 G was used for Q.[20] For ρ_c we again take one-half of the square of the coefficient of the $C\text{-}2p_z$ atomic orbital in the HOMO so that $A_\pi = -28C_{\pi i}^2/2$.

Scheme III

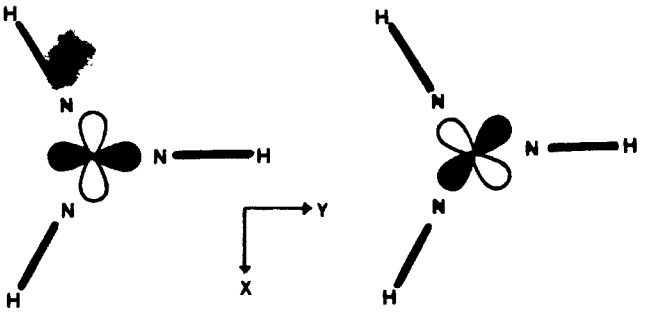

Substitution of the values of A_σ and A_π calculated as described above then gives the contact shifts of the proton signals in the NMR caused by σ- and π-delocalization, respectively, of the unpaired electron onto the pyrazole rings. The sum of the two contributions gives the net Fermi contact shift. These values are collected in Table XII. Positive $\Delta\delta$ correspond to upfield shifts.

The calculations suggest that H_5 is shifted the farthest upfield, followed by H_3 and then H_4. Therefore, the observed resonances at δ −18.8, −8.5, and +3.1 are assigned to H_5, H_3, and H_4 in that order. To get an experimental paramagnetic shift, average chemical shifts of a variety of diamagnetic $TpMo(CO)_nL_m$ complexes were taken as the chemical shifts of a hypothetical, diamagnetic $TpMo(CO)_3$. These average chemical shifts for the H_5, H_4, and H_3 protons were found to be 7.0, 6.2, and 7.2 ppm. The $\Delta\delta$(obsd) listed in Table XII is then the difference between these values and the chemical shifts observed for $TpMo(CO)_3$.

The agreement between the calculated $\Delta\delta$(net) and $\Delta\delta$(obsd) is embarassingly good given the level of the theoretical treatment and the fact that any pseudocontact (dipolar) shift has been neglected. The pseudocontact (pc) shift for an axial system is given by[17,18]

$$\frac{\Delta H}{H} = \frac{-g\beta^2 S(S+1)}{9kT}\left(\frac{3\cos^2\theta - 1}{r^3}\right)(g_\parallel^2 - g_\perp^2)$$

The geometrical factor $(3\cos^2\theta - 1)/r^3$ is accurately known from the structure, but the difference $g_\parallel^2 - g_\perp^2$ must be determined from the ESR spectrum. At ca. 90 K, a strong signal is observed for **1** in frozen THF.[21] The estimated parameters from the spectrum are $g_\perp = 1.93$, $g_\parallel = 1.92$, $A_\perp \simeq 35$ G, $A_\parallel \approx 7$–10 G (here the hyperfine coupling constants, $A_\parallel$, $A_\perp$, refer to the splittings from the Mo isotopes with spin = $^5/_2$). With these values for $g_\parallel$ and $g_\perp$, and pc shifts calculated for H_5, H_4, and H_3 are −0.10, +0.02, and +0.32, respectively. These small pc shifts are negligible compared to the Fermi contact shifts.

(17) Carrington, A.; McLachlan, A. D. *Introduction to Magnetic resonances*; Harper and Row: New York, 1967.
(18) LaMar, G. N.; Horrocks, W. DeW., Jr.; Holm, R. H., Eds.; *NMR of Paramagnetic Molecules*; Academic Press: New York, 1973.
(19) McConnell, H. M.; Chesnut, D. M. *J. Chem. Phys.* **1956**, *25*, 890.
(20) Curtis, M. D.; Allred, A. L. *J. Am. Chem. Soc.* **1965**, *87*, 2554.
(21) In our preliminary communication, a g-value of 1.98 was assigned to $TpMo(CO)_3$ in solution at room temperature. The very weak signal observed probably is not due to **1** in view of the fact that if the relaxation times are appropriate for observing ^{1}H NMR, the ESR cannot be observed and vice versa (see ref 17, 18).

Scheme IV

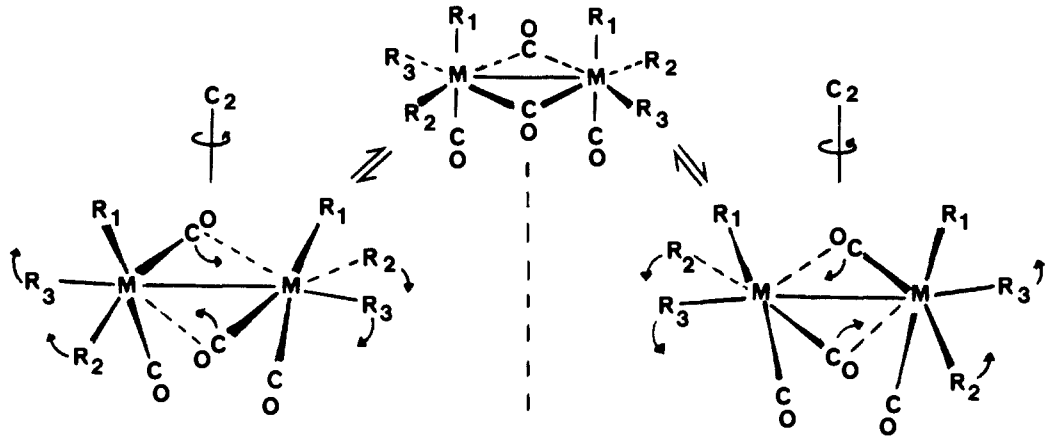

However, we are caught on the horns of a dilemma. The ESR result shows a small g-anisotropy as required if the observed paramagnetic shifts are determined primarily by the Fermi contact mechanism. Yet, the same EHMO calculation which gives such good agreement with the contact shifts also demands a large g-anisotropy. The ground state predicted for the $(3a_1)^2(6e)^3$ configuration is ^2E. This state is split by spin–orbit coupling into two Kramer's doublets separated by $2K^2\lambda$ (K = orbital reduction factor). The lower Kramer's doublet is calculated to have $g_\parallel$ = 5.6, $g_\perp$ = 1.7 and thus resembles the magnetic behavior of the ferricenium ion, Cp_2Fe^+, which also has an $(a_1)^2(e)^3$ configuration with $g_\parallel$ = 4.36 and $g_\perp$ = 1.30.[22-24]

It is possible that a dynamic Jahn–Teller effect is responsible for the reduction of the orbital contribution to the g-anisotropy.[25] If this is the case, then the g-anisotropy might become evident at temperatures ≤4 K. Such studies are planned and will be reported separately. In any event, the observed ESR spectrum is similar to that reported for $Tp^*Mo(NO)(NCMe)_2^+$ and some Mo(V) complexes.[26] Regardless of the mechanism by which the orbital angular momentum associated with the E ground state is quenched, the results strongly suggest that the observed paramagnetic shifts are due to the Fermi contact term and that π-delocalization is by far the dominant mechanism for placing spin density at the ring protons.

Structure of 1. The structure of **1** is shown in Figures 2 (Ortep plot) and 3 (space-filling model). Bond distances and angles are in Table IV. In the solid, the molecule has imposed C_3 symmetry, but the symmetry of the molecule hardly deviates from C_{3v}. As Figure 3 shows, the structure is rather crowded. The maximum cone angle of the Tp ligand is calculated to be ca. 180° from the structural data and thus covers one-half of the metal coordination sphere. For comparison, we have calculated the cone angles of Cp and Cp* to be 100 and 146°.

The bond distances and angles in the Tp ligand are unremarkable. The Mo–CO distance, 2.01 (1) Å, is slightly longer than the terminal Mo–CO distance (1.96 [1] Å)[27] in $Tp_2Mo_2(CO)_4$ (see below) or $Tp^*Mo(CO)_3^-$ (Tp^* = $HB(3,5\text{-}Me_2HC_3N_2)_3$) (1.941 [4] Å).[28] The increase in the Mo–CO length over that in the anion may be ascribed to increase d → π^* bonding in the latter. As expected, the C–O distances are longer (1.167 [5] Å)

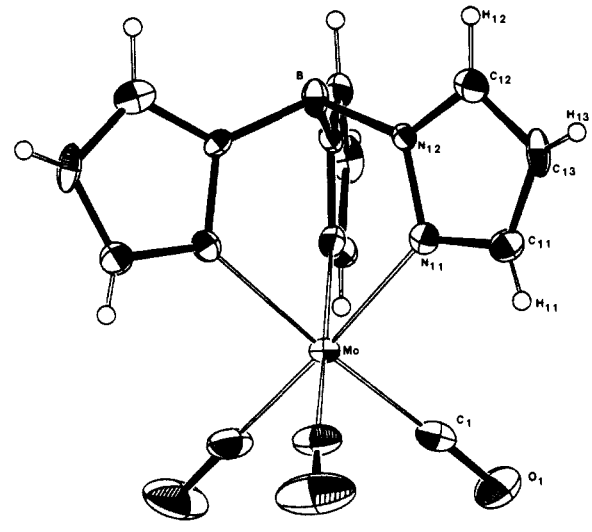

Figure 2. Ortep drawing of $TpMo(CO)_3$ (**1**). Thermal ellipsoids are drawn at the 50% probability level.

in the anion than in the neutral radical (1.13 (1) Å).

$Tp_2Mo_2(CO)_4(Mo{\equiv}Mo)$ (2). Synthesis. Compound **2** is prepared in good yield by the thermolysis of performed **1** or, in one operation, by heating a mixture of the anion, $TpMo(CO)_3^-$, and an oxidizing agent, preferably Cp_2Fe^+, according to eq 2. The

$$2TpMo(CO)_3^- \xrightarrow{-2e^-} \underset{\mathbf{1}}{2TpMo(CO)_3} \xrightarrow[\Delta]{-2CO} \underset{\mathbf{2}}{Tp_2Mo_2(CO)_4} \quad (2)$$

formation of **2** thus parallels the synthesis of $Cp_2Mo_2(CO)_4(Mo{\equiv}Mo)$ (**3**) by thermolysis of $Cp_2Mo_2(CO)_6$.[11,15] Although $Cp_2Mo_2(CO)_6$ dissociates into the radical, $CpMo(CO)_3$, at the temperatures necessary to induce CO loss, recent results indicate this homolytic dissociation is not involved in the formation of the triply bonded dimer (**3**).[29] Nevertheless, the mixed dimer, $Cp_2MoW(CO)_4(Mo{\equiv}W)$, may be obtained from the thermolysis of a mixture of $Cp_2Mo_2(CO)_6$ and $Cp_2W_2(CO)_6$.[11] We, therefore, sought the synthesis of the mixed ligand dimer, $Tp(CO)_2Mo{\equiv}Mo(CO)_2Cp$, by heating a mixture of $TpMo(CO)_3$ and $Cp_2Mo_2(CO)_6$. Furthermore, if the formation of **2** proceeds through the 15-electron species, $TpMo(CO)_2$ (**4**), this species might be trapped by $Cp_2Mo_2(CO)_4$ to give a trimer, e.g., **5**.

$$\underset{\mathbf{1}}{TpMo(CO)_3} \xrightarrow[\Delta]{-CO} \underset{\mathbf{4}}{TpMo(CO)_2} \xrightarrow{\frac{3}{2}} \underset{\mathbf{5}}{Cp(CO)_2Mo{=}Mo(CO)_2Cp} \quad (3)$$

(22) Prins, R.; Reinders, F. J. *J. Am. Chem. Soc.* **1969**, *91*, 4929.
(23) Solodovnikov, S. D. *Russ. Chem. Rev.* **1982**, *51*, 961.
(24) Ammeter, J. H. *J. Magn. Reson.* **1978**, *30*, 299.
(25) (a) Bersuker, I. B. *The Jahn–Teller Effect and Vibronic Interactions in Modern Chemistry*; Plenum Press: New York, 1984. (b) Höchli, U. T. *Phys. Rev.* **1967**, *162*, 262.
(26) (a) Atherton, N. M.; Denti, G.; Ghedini, M.; Oliva, C. *J. Magn. Reson.* **1981**, *43*, 167. (b) Manoharin, P. T.; Rogers, M. T. *J. Chem. Phys.* **1968**, *49*, 5510. (c) McGarvey, B. R. *Inorg. Chem.* **1966**, *5*, 476.
(27) Standard deviations from the least-squares variance–covariance matrix are reported in parentheses. Standard deviations for averaged values are calculated by the $n-1$ formula and are reported in square brackets.
(28) Marabella, C. D.; Enemark, J. H. *J. Organomet. Chem.* **1982**, *226*, 57.
(29) Turaki, N. N.; Huggins, J. M. *Organometallics* **1985**, *4*, 1766.

$$Cp_2Mo_2(CO)_6 \xrightarrow[\Delta]{} CpMo(CO)_3 \xrightarrow[-2CO]{I} Tp(CO)_2Mo{\equiv}Mo(CO)_2Cp \quad (4)$$

Heating a mixture of **1** and **3** in toluene to reflux for 2 h gave no detectable reaction. This was surprising since **1** is partially converted to **2** within 10 min in refluxing acetonitrile. Apparently the acetonitrile assists the CO dissociation from **1**. Heating a mixture of **1** and $Cp_2Mo_2(CO)_6$ in toluene to reflux showed only the conversion of the singly bonded dimer to **3**. Since $CpMo(CO)_3$ is formed under these conditions, the combination of the $CpMo(CO)_3$ and $TpMo(CO)_3$ radicals must not be favored, at least at 110 °C, in keeping with the apparent preference for the TpMo group to be six-coordinate.[5]

$TpMo(CO)_3^-$ was allowed to react with $CpMo(CO)_3BF_4$ in an alternate attempt to prepare the mixed ligand dimer, $Tp(CO)_3Mo{-}Mo(CO)_3Cp$. The only products identified were $Cp_2Mo_2(CO)_6$ and $TpMo(CO)_3$. A one-electron oxidation of the anion by the cation is indicated:

$$TpMo(CO)_3^- + CpMo(CO)_3^+ \rightarrow TpMoCO)_3 + [CpMo(CO)_3\cdot] \rightarrow {}^1/_2Cp_2Mo_2(CO)_6 \quad (5)$$

Structure of 2. The molecular structure of **2** is shown in Figure 4. The structure has more similarities to that of $Cp^*_2Mo_2(CO)_4$ (**6**)[3c] than to that of $Cp_2Mo_2(CO)_4$ (**3**).[30] Thus, the Tp–Mo–Mo–Tp axis[31] is bent (ω = 153.4 [9]) as in **6** (ω = 168°) whereas **3** has a linear (ω = 180°) Cp–Mo–Mo–Cp axis. The Mo≡Mo bond length in **2** is 2.507 (1) Å compared to 2.488 (3) and 2.448 (1) Å in **6** and **3**. In fact, the Mo≡Mo bond lengths seem to correlate with the cone angle of the ligand, L, in these $L_2Mo_2(CO)_4$ compounds. The differences in the Mo≡Mo bond lengths are (L(cone angle)) the following: Tp(180°)–Cp(100°) = 0.06 Å, Cp*(146°)–Cp(100°) = 0.04 Å, and Tp(180°)–Cp*(146°) = 0.03 Å.

There is an approximate C_2 axis which bisects the Mo≡Mo bond and the N_{211}–Mo–Mo–N_{121} dihedral angle. This symmetry may be seen in the view presented in Figure 5. In C_2 symmetry, the carbonyls are divided into two sets: {C_{11}–O_{11}, C_{21}–O_{21}} (set 1) and {C_{12}–O_{12}, C_{22}–O_{22}} (set 2). The symmetry related N donors are grouped into three sets: {N_{111}, N_{231}}, (set 3), {N_{131}, N_{221}} (set 4), and {N_{121}, N_{211}} (set 5). The N atoms in set 3 are approximately trans to the Mo≡Mo bond, while those in sets 4 and 6 are cis to it and more or less trans to the carbonyls.

The carbonyl groups in set 1 are semibridging (Mo′–Mo–C = 70.5 [1.5]°) and have shorter Mo–C bonds (1.93 [1] Å) than set 2 (Mo′–Mo–Co = 83.4 [4]°, Mo–C = 1.96 [1] Å). The asymmetry parameter (α)[32,33] and the M–C–O angle (θ) for sets 1 and 2 are (α, θ) (0.27, 171°) and (0.41, 175°) and are consistent with semibridging and terminal carbonyls, respectively. As in **3**, the semibridging carbonyls are essentially linear in contrast to the more usual bent semibridges.[33] This linear mode of semibridging has been attributed to a π-donor interaction of the filled carbonyl π-orbital with a vacant π- or π^*-acceptor orbital on the metal.[30,32,33] Recently, Hall and co-workers have advanced an alternate explanation for the linear bonding mode.[34] In their model, all semibridging carbonyls are π-acceptors and the M–C–O angle is determined by the nature of the metal-donor orbital, usually the HOMO of the metal–metal bond. For M≡M multiple bonds, the HOMO is normally the M–M π-orbital, and the semibridging carbonyl is linear. If the HOMO is a π^*-orbital (usual for M–M single bonds), the semibridge is bent.

The pattern of the semibridging interactions in **2** closely resembles the pattern found in $Cp^*_2Mo_2(CO)_4$.[3c] In these two compounds only two of the four carbonyls are semibridging. In $Cp_2Mo_2(CO)_4$ (**3**), $Cp_2Cr_2(CO)_4$,[35] and $(indenyl)_2Mo_2(CO)_4$[36] all four carbonyls are semibridging. The latter two compounds have bent L–M–M–L axes. Therefore, there is no correlation between the number of bridging carbonyls and the L–M–M angle although a correlation might have been anticipated on a theoretical basis.[37] It is probable that there is a soft energy surface for the bridge ↔ terminal interchange and L–M–M–L deformation.[11,37] The softeness of the energy surface for deformation of the $Tp_2Mo_2(CO)_4$ structure is shown by its fluxional behavior in solution.

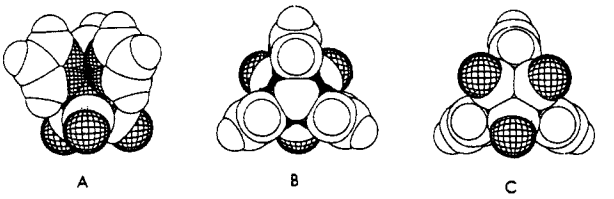

Figure 3. Space-filling drawings of $TpMo(CO)_3$: (A) perpendicular to the C_3 axis, (B) down the B → Mo vector, (C) down the Mo → B vector.

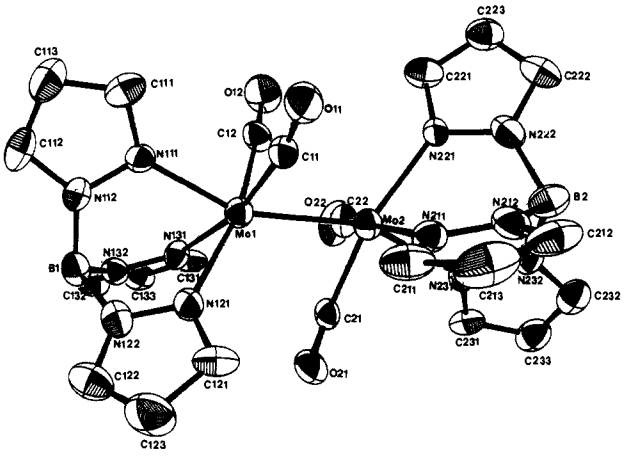

Figure 4. Ortep drawing of $Tp_2Mo_2(CO)_4$.

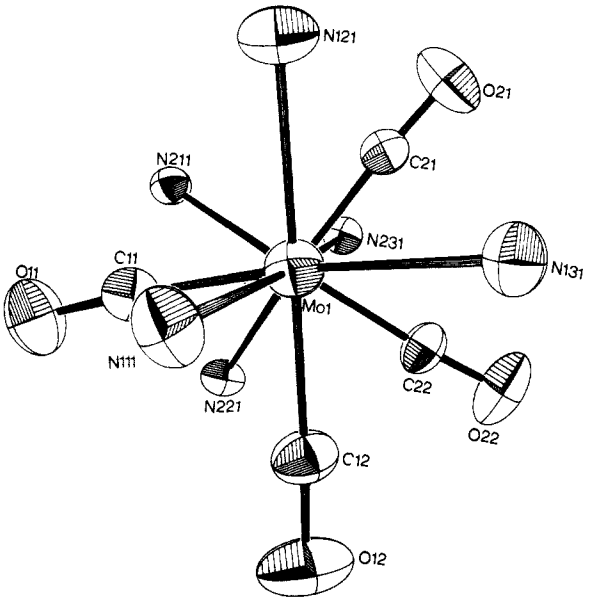

Figure 5. Ortep drawing of the inner coordination sphere of $Tp_2Mo_2(CO)_4$. The view is along the Mo_1 → Mo_2 vector. An approximate C_2 axis bisects the Mo–Mo bond and the N_{121}–Mo_1–Mo_2–N_{211} dihedral angle.

(30) Klingler, R. J.; Butler, W. M.; Curtis, M. D. *J. Am. Chem. Soc.* **1978**, *100*, 5034.
(31) In reporting angles, Tp refers to the centroid of the coordinates of the three N donor atoms.
(32) Curtis, M. D.; Han, K. R.; Butler, W. M. *Inorg. Chem.* **1980**, *19*, 2096.
(33) Horwitz, C. P.; Shriver, D. F. *Adv. Organomet. Chem.* **1984**, *23*, 219–305.
(34) Morris-Sherwood, B. J.; Powell, C. B.; Hall, M. B. *J. Am. Chem. Soc.* **1984**, *106*, 5079.
(35) Curtis, M. D.; Butler, W. M. *J. Organomet. Chem.* **1978**, *155*, 131.
(36) Bakkar, I.; Curtis, M. D.; D'Errico, J. J., unpublished results.
(37) Jemmis, E. D.; Pinhas, A. R.; Hoffman, R. *J. Am. Chem. Soc.* **1980**, *102*, 2576.

Fluxional Behavior of 2. As discussed above, the solid-state structure of **2** has approximate C_2 symmetry. In this symmetry, there are two sets of carbonyls and three inequivalent sets of pyrazole rings on the Tp ligands. From room temperature to −80 °C, however, the ^{13}C NMR and ^1H NMR spectra of **2** show only two types of nonequivalent pyrazole rings in a 2:1 ratio, although the two sets of carbonyl carbons exhibit two singlets in the ^{13}C NMR as expected. We propose that the enantiomers of **2** rapidly interconvert as shown in Scheme IV. In this mechanism, the semibridging carbonyls undergo pairwise exchange with synchronous rotation of rings R_2 and R_3 more or less about the M–R_1 axis. This motion leads to an intermediate of C_{2v} symmetry which may collapse to either enantiomer. This process averages the magnetic environments of rings R_2 and R_3 and leaves R_1 distinct. Thus, the "B" resonances (see Experimental Section) are assigned to rings R_2 and R_3 (sets 3 and 4 as defined above) and the "A" resonances to R_1 (set 5). The semibridging and terminal carbonyl environments are not interchanged so that the carbonyl sets 1 and 2 remain distinct. It is interesting to note that in $Cp_2MoW(CO)_4$, all four semibridging carbonyls exchange metal sites on the NMR time scale.[11]

Reactivity of 1 and 2. Only a very limited number of reactions of the radical **1** have been attempted. Compound **1** reacts with diazoalkanes, but the products have not been identified as yet. Elemental sulfur or propylene sulfide gave compound **7**.

$$2TpMo(CO)_3 + S \xrightarrow{-2CO} \underset{\mathbf{7}}{Tp(CO)_2Mo{\equiv}S{\equiv}Mo(CO)_2Tp} \quad (6)$$

The reactivity of $Tp_2Mo_2(CO)_4$ (**2**) toward nucleophiles is drastically reduced as compared to $Cp_2Mo_2(CO)_4$ (**3**).[2] Compound **2** does not react with acetylenes (C_2H_2, PhCCH, EtCCH), Ph_2CN_2, CH_2N_2, or $P(OMe)_3$. Even CO does not react with **2** at 1 atm of pressure. A prolonged reaction of **2** with CO (172 atm, 35 °C, 3 days) gave $Mo(CO)_6$ as the only carbonyl containing product. Compound **3** reacts very rapidly at <25 °C with all the above reagents.[2]

No reaction between **2** and S_8 or propylene sulfide was observed even after prolonged reflux in toluene. Compound **3** reacts rapidly with these reagents even at 0 °C.[38] No reaction was observed with H_2 (172 atm, 35 °C, 1 day) or with Cp_2Fe^+. HCl and **2** in refluxing acetonitrile reacted to give a complex mixture.

In its reactions with I_2 and Br_2, **2** resembles $Cp^*_2Mo_2(CO)_4$.[3] The Mo≡Mo bond is cleaved and CO transfer occurs to give the tricarbonyl halides

$$Tp_2Mo_2(CO)_4 + X_2 \rightarrow TpMo(CO)_3X + \ldots \quad (7)$$

(X = Br, I)

Sodium reduces **2** to the $TpMo(CO)_3^-$ anion as the major product. This behavior is found with **3** and **6** also. In summary, the reactivity of the Mo≡Mo bond in **2** is drastically reduced compared to the Cp and even the Cp* analogues.

Conclusions. The Tp ligand, while grossly resembling Cp in its electronic interaction with metals, strongly prefers a six-coordinate environment in its Mo complexes. The large cone angle (ca. 180°) may be responsible for this preference, but electronic effects may also play an important role.[5] The preference for six-coordination makes possible the stabilization of $TpMo(CO)_3$ and $Tp_2Mo_2(CO)_4(Mo{\equiv}Mo)$ relative to the unknown seven-coordinate single bonded dimer, $Tp_2Mo_2(CO)_6$. The steric bulk of the Tp ligand may also inhibit **2** from undergoing reactions characteristic of the Mo≡Mo bond in $Cp_2Mo_2(CO)_4$.

Acknowledgment. We thank the National Science Foundation for support of this research (Grant No. CHE-8206153). K.-B.S. is also grateful for a James E. Harris Fellowship and Rackham Graduate Fellowship. We also thank Professors M. B. Hall, J. H. Enemark, J. M. Huggins, and F. J. Lalor for communication of results prior to publication.

Appendix

The EHMO calculations were performed with R. Hoffmann's programs ICON8 and FMO with the weighted H_{ij} option.[39] The bond lengths and angles were those determined experimentally except all C–H and B–H bonds were set to 1.0 Å, and the coordinates were idealized to strict C_{3v} symmetry. The atom parameters used have been tabulated[40] with the exception of those for B which were the standard ones contained in the program: $H(2s) = -15.2$ eV, $H(2p) = -8.5$ eV, $\zeta = 1.300$.

Registry No. 1, 85803-21-0; **2**·$CHCl_3$, 85803-20-9; **3**, 56200-27-2; $[Et_4N][TpMo(CO)_3]$, 16970-22-2; Cp_2FePF_6, 11077-24-0; $[CpMo(CO)_3]BF_4$, 75763-80-3; $Cp_2Mo_2(CO)_6$, 12091-64-4; $Na[TpMo(CO)_3]$, 101859-86-3; $TpMo(CO)_2(\eta^2\text{-COMe})$, 86822-12-0; $TpMo(CO)_3I$, 95156-35-7; $TpMo(CO)_3Br$, 86822-13-1; $Mo(CO)_6$, 13939-06-5; Na, 7440-23-5; CH_3I, 74-88-4; I_2, 7553-56-2; Br_2, 7726-95-6; CO, 630-08-0; PhC≡CH, 536-74-3; EtC≡CH, 107-00-6; $P(OMe)_3$, 121-45-9; H_2, 1333-74-0; Ph_2CN_2, 883-40-9; HCl, 7647-01-0; $[TpMo(CO)_2]_2S$, 95156-30-2; S_8, 10544-50-0; $CpMo(CO)_3$, 12079-69-5; Mo, 7439-98-7; propylene sulfide, 1072-43-1.

Supplementary Material Available: Tables III and VII (thermal parameters for **1** and **2**, respectively), Tables V and X (listing of F_o vs. F_c for **1** and **2**), Table IX (equations of planes for **2**) (18 pages). Ordering information is given on any current masthead page.

(38) Curtis, M. D.; Butler, W. M. *J. Chem. Soc., Chem. Commun.* **1980**, 998.

(39) Ammeter, J. H.; Burgi, H.-B.; Thibeault, J. C.; Hoffman, R. *J. Am. Chem. Soc.* **1978**, *100*, 3686.

(40) Curtis, M. D.; Eisenstein, O. *Organometallics* **1984**, *3*, 887.